Journal of ELECTRONIC MATERIALS, Vol. 45, No. 3, 2016
DOI: 10.1007/s11664-015-4022-z
© 2015 The Minerals, Metals & Materials Society

Investigation of Barrier-Layer Materials for Mg_2Si/Ni Interfaces

TATSUYA SAKAMOTO,[1,3] YUTAKA TAGUCHI,[1] TAKESHI KUTSUWA,[2] KIYOHIDE ICHIMI,[2] SHINICHI KASATANI,[2] and MINORU INADA[2]

1.—R&D Div., Yasunaga Corporation, 3-4-1 Kamezawa, Sumida, Tokyo 130-0014, Japan.
2.—R&D Div., Yasunaga Corporation, 3860 Midorigaoka-Nakamachi, Iga, Mie 518-0834, Japan.
3.—e-mail: sakamoto-tab@fine-yasunaga.co.jp

The durability of Ni electrodes, which are often used for Mg_2Si thermoelectric chips, is poor at high working temperatures because of deposition of Mg at the Mg_2Si/Ni interface and on the surface. Hence, a "Mg_2Si/barrier material/Ni" structure was adopted instead of direct adhesion of Ni to Mg_2Si. Ti, $TiSi_2$, and TiN were selected as candidate materials for the barrier layer between Mg_2Si and Ni, and the barrier effect, adhesion, and contact resistance of each of these materials were evaluated. After the samples had been annealed at 873 K for 1 h, Mg appeared on the Ti surface and $TiSi_2$ deposited on Mg_2Si; however, no Mg was detected on the surface of TiN or in the inner part of the Ni electrode. Continuous, low contact resistance was also observed for Mg_2Si/TiN/Ni samples. TiN does not adhere strongly to Mg_2Si but is a promising barrier material for Mg_2Si/Ni interfaces.

Key words: Magnesium silicide, electrode, diffusion barrier layer

INTRODUCTION

Waste heat recovery in the middle-to-high temperature range by use of thermoelectric (TE) materials has been developed as technology for reducing fuel consumption. In particular, silicides, skutterudites, and half-Heusler compounds are attractive materials because of their promising TE properties. Yasunaga Corporation has researched and developed TE materials and chips based on magnesium silicide (Mg_2Si), which is abundant in the Earth's crust and is of low toxicity.[1]

TE chips are preferably attached strongly to a metal electrode, because metal electrodes are easily soldered and/or brazed. In addition, the contact resistance of the electrode obtained should be low ($<10\ \mu\Omega\ cm^2$)[2] and its performance should be constant up to 10,000 h at its operating temperature, e.g., 823 K. (In Japan, the average vehicle is used for approximately 13 years[3] and average usage is 2 h/day). Therefore, the properties required for electrodes are high adhesion, low contact resistance, and long-term durability. An important aspect of satisfying these requirements is the choice of electrode material and the forming process, which should be selected such that the electrode material does not deteriorate at the operating temperature and no diffusion or chemical reaction occurs between the electrode material and Mg_2Si.

We have developed a diffusion-bonding technique with spark plasma sintering (SPS) for fabrication of Ni electrodes on Mg_2Si substrates; however, we have observed that a chemical reaction between Ni and Mg_2Si in these electrodes generates Ni–Si alloys and metallic Mg. If the Ni/Mg_2Si interface formed by diffusion bonding is subjected to high operating temperatures for an extended period, Mg is oxidized at the Ni/Mg_2Si interlayer. Although our diffusion bonding method is effective for adhesion, it generates Mg and becomes disadvantageous with regard to durability. In addition, the difficulty of quantity control of diffusion during SPS is also expected to be problematic, as it is for the monobloc sintering method.[2,4]

We therefore used sputtering, a dry plating method, because it results in much less diffusion than the conventional method. In this study we identified a suitable barrier material for insertion between the Ni electrode and Mg_2Si substrate that would result in less diffusion.

(Received June 1, 2015; accepted August 27, 2015; published online September 14, 2015)

For insertion of a barrier material, i.e., "Mg_2Si/barrier material/Ni," which is less chemically reactive than Ni when adhering directly to Mg_2Si, we considered three candidate materials.

Ti

The diffusion coefficient of Ni in Si is 0.1 cm^2/s at 723–1073 K[5] and the diffusion coefficient of Ti in Si ranges from 5×10^{-10} cm^2/s to 10^{-8} cm^2/s at 1223–1473 K;[6] thus, Ti seems less diffusive than Ni in Si. Therefore, we expected the chemical reaction between Mg_2Si and Ti to be inhibited. Even if Ti and Mg_2Si react and generate $TiSi_2$ and Mg, Mg does not move into the Ti layer (according to the Ti–Mg phase diagram[7]). In addition, although Ni is known for its rapid diffusion in Ti, the solubility limit of Ni in Ti is quite small.[8] Furthermore, Ti is used as an adhesive layer between semiconductor Si and Ni electrodes for power devices, where its adhesion and Ohmic contact are good. This characteristic is also preferable for Mg_2Si.

$TiSi_2$

Stable metal silicides prepared by combining a metal and silicon are often used to reduce the contact resistance of semiconductor Si electrodes. We hypothesized that if the Si composition x of a metal silicide MSi_x is saturated at the upper limit, Si would not diffuse from Mg_2Si. WSi_2, $TiSi_2$, $CoSi_2$, and NiSi are widely used as silicide materials; we selected $TiSi_2$ because of its low resistivity, linear coefficient of expansion similar to that of Mg_2Si, durability at working temperatures, possibility of removing native oxides, easy controllability of composition, and low material cost.[9–12]

TiN

Titanium nitride (TiN) is used as a diffusion barrier layer for Si semiconductor devices.[13–16] It is also expected to serve as a barrier layer for Mg.

Electrodes consisting of a combination of an Mg_2Si substrate and a Ni electrode were also fabricated for reference purposes.

EXPERIMENT 1: EVALUATION OF THE BARRIER EFFECT FOR THE CANDIDATE MATERIALS

For sample preparation, Mg_2Si was synthesized by use of an all-molten method and subsequently sintered by SPS in-house. Details of the method are reported elsewhere.[17] Sintered pellets were sliced to a thickness of 2 mm by use of a multi-wire saw (SW-1520; Yasanuga); the surfaces of these pellets were then polished to a mirror finish.

The candidate materials were deposited on to Mg_2Si substrates by use of a carousel-type sputtering machine (SPC-1000W; Showa Shinku). The base pressure was 0.4 Pa. The argon gas flow rate was 10 sccm during sputtering. A DC power supply with an output of 800 W or 600 W was used as power source for sputtering $TiSi_2$, Ti, TiN, and Ni.

Film thickness was controlled via sputtering time, and films as thick as 200 nm were deposited. Ni electrodes were not deposited on to the barrier candidate materials because the purpose of these experiments was to evaluate the barrier effect against Mg_2Si. Samples were annealed at 873 K for 1 h under an Ar atmosphere. During annealing, pieces of quartz glass were placed on both sample surfaces to prevent adhesion of foreign substances (contamination) that might be scattered from the Mg_2Si substrate. The annealed substrates were then cut to dimensions 2 mm wide × 2 mm deep by use of the wire saw.

The surfaces of the annealed samples were observed with a laser microscope (VK-X210, Keyence). The laser wavelength was 408 nm, the objective lens magnification was 50×, and resolution in the height direction was 0.1 nm.

Figure 1 shows the surface depth analysis images for (a) Ni (b) Ti (c) $TiSi_2$, and (d) TiN. The images in column 1 in Fig. 1 are the images of samples not subjected to annealing, whereas those in the column 2 are the images of samples annealed at 873 K for 1 h. As shown in Fig. 1a and b, the annealed Ni and Ti films were rough and appeared to be broken along a grain boundary. These features were apparently caused by mismatch of the coefficients of thermal expansion (CTE) of the Ni/Ti films and Mg_2Si and/or by recrystallization of Ni/Ti. The CTE of Ni and Ti at room temperature are 13.5×10^{-6}/K and 8.4×10^{-6}/K, respectively.[18] These values are smaller than the CTE of Mg_2Si (16.5×10^{-6}/K, measured in-house); thus, Ni and Ti seem to be expanded by Mg_2Si during annealing.

As shown in Fig. 1c, the surface of $TiSi_2$ also appears rougher than before annealing. However, this film appears to be less damaged than the Ni and Ti films.

The TiN surface appears to not be broken after being annealed, despite the TiN CTE being 9.4×10^{-6}/K,[19] which is smaller than the Ni CTE. TiN is a hard material; therefore, it is used as a coating in the fabrication of super-hard materials. In particular, it does not appear prone to cracking owing to its CTE mismatch with Mg_2Si.

The effect of annealing at 873 K for 1 h on the composition of the deposited materials was estimated by use of x-ray photoelectron spectroscopy (XPS). XPS was performed with a Quantam 2000 (ULVAC-PHI) equipped with an Al–Kα x-ray source. The measurement resolution was 1 eV for wide scanning. Before being scanned, the sample surfaces were cleaned by being sputtered with a 2-keV Ar^+-ion beam for 5 min to remove native oxides and contaminants; the rate of etching of SiO_2 was 4 nm/min.

Figure 2 shows the XPS spectra of Ni, $TiSi_2$, Ti, and TiN films on Mg_2Si substrates, after annealing

Fig. 1. Height images of the deposited films. The images in column 1 show the surfaces of films not subjected to annealing, whereas those in column 2 show surfaces of films annealed at 873 K for 1 h. (a-1) Ni without annealing, (a-2) Ni annealed at 873 K for 1 h, (b-1) Ti without annealing, (b-2) Ti annealed at 873 K for 1 h, (c-1) $TiSi_2$ without annealing, (c-2) $TiSi_2$ annealed at 873 K for 1 h, (d-1) TiN without annealing, (d-2) TiN annealed at 873 K for 1 h.

of the samples at 873 K for 1 h. Figure 2a and b show the ranges from 0 eV to 1200 eV and from 200 eV to 400 eV, respectively. As shown in Fig. 2b, peaks were observed at approximately 301 eV in the spectra of the Ni, $TiSi_2$, and Ti samples; the intensity of these peaks in the spectra of Ni and $TiSi_2$, in particular, were stronger than that in the spectrum of Ti. A KLL peak of Mg metal appeared at 301 eV; thus, the peaks observed at approximately 301 eV were attributed to Mg. However, no clear peak at approximately 301 eV was observed in the spectrum of the TiN films.

Two hypotheses were considered to explain formation of the Mg observed on the Ni, $TiSi_2$, and Ti films:

1. chemical reaction between the deposited material and Mg_2Si; and/or

$$\text{Deposited metal} + Mg_2Si \rightarrow \text{Metal-silicide} + 2Mg \quad (1)$$

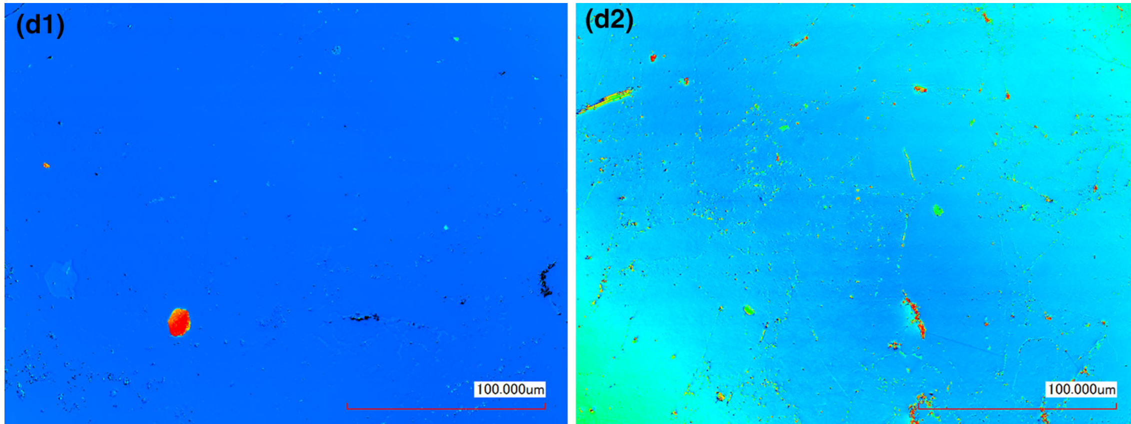

Fig. 1. continued.

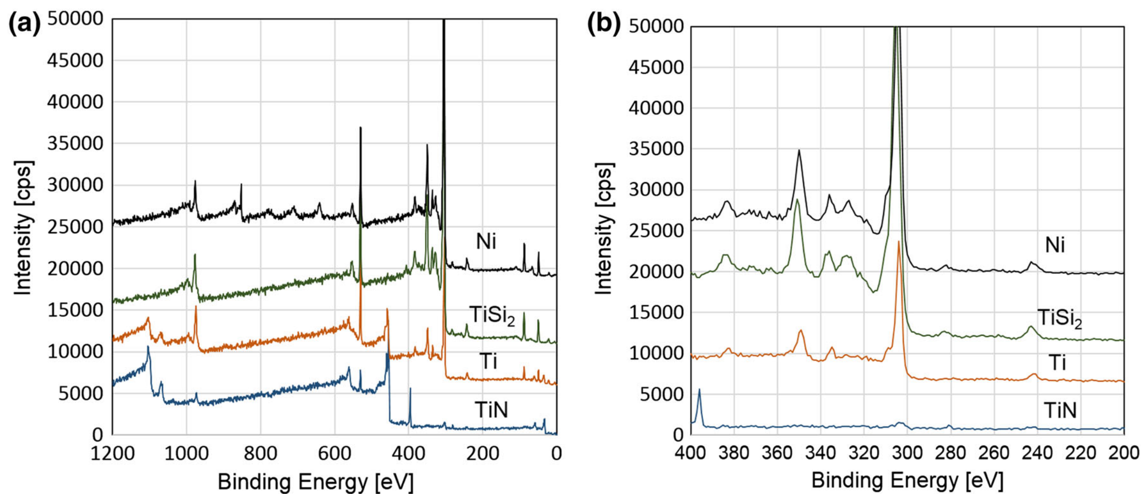

Fig. 2. X-ray photoelectron spectra of Ni, $TiSi_2$, Ti, and TiN films on Mg_2Si substrates; the samples were annealed at 873 K for 1 h. (a) and (b) show the ranges from 0 eV to 1200 eV and from 200 eV to 400 eV, respectively.

2. thermal decomposition of Mg_2Si.

$$Mg_2Si \rightarrow 2Mg + Si \quad (2)$$

To understand the distribution of Mg, compositional depth profiles were obtained by XPS in conjunction with Ar^+-ion etching. The etching rate was approximately 8.4 nm/min for SiO_2 and 4 nm/min for Ti.

Figure 3 shows the XPS depth profiles of (a) Ni, (b) Ti, and (c) TiN films. As shown in Fig. 3c, Mg was not observed during the entire etching time for the TiN film. In contrast, Fig. 3a and b shows the distribution of Mg throughout the film; the density of Mg was particularly high at the surface.

As shown in Fig. 1a-2 and b-2, cracks in the films were observed. Mg appears to be present in the cracks, and occasionally throughout the films. The reason for the high density of Mg at the surface is illustrated in Fig. 4. The generated Mg tended to accumulate between the quartz glass and the deposited film and then to become deposited on the film.

The TiN film seems to be more resistant to cracking than the other films; thus, it might function well as a barrier material.

EXPERIMENT 2: EVALUATION OF ADHESION

To study the adhesion of TiN, peeling tests were performed. Formed TiN surfaces were attached to a piece of VHB KPP-19 (3M) tape then removed from the tape; this process was performed 10 times.

Table I shows the results of the peeling test. As shown in this table, TiN was easily stripped from samples after annealing at 823 K for 100 h under an Ar atmosphere. Countermeasures are required because TiN was easily peeled off.

Fig. 3. XPS depth profiles for (a) Ni, (b) Ti, and (c) TiN films.

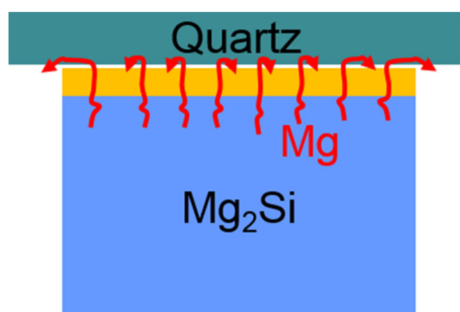

Fig. 4. Schematic diagram of Mg deposition on a film surface.

EXPERIMENT 3: EVALUATION OF CONTACT RESISTANCE

Although we have discussed the appearance of Mg in Experiment 1, we performed contact resistance measurement between the formed material and Mg_2Si to understand the effect of Mg better. In this experiment, a 200-nm-thick Ni film was deposited on to a barrier candidate material which was, in turn, deposited on to Mg_2Si. The chip size was $2 \times 2 \times 2$ in mm^3. Contact resistance measurements were performed on three chips and the average and standard deviation of the three measurements were calculated. Measurements were obtained by use of a home-made device, “RM-0” (more information is given in the Appendix). Resistance was measured by use of a Hioki BT3562 AC-type resistance-measurement system connected to the RM-0. The measurement principle and equipment were the same as described elsewhere.[2]

Figure 5 shows the contact resistance measurement results before and after annealing of the samples at 873 K for 1 h under Ar. The contact resistance of the TiN/Ni electrode increased only slightly after the sample had been annealed. For the

Table I. Peeling test results before and after the durability test at 823 K for 100 h

Initial condition	Annealing condition before peeling test	Before durability test		After annealing at 823 K, 100 h in Ar	
		Successful	Unsuccessful	Successful	Unsuccessful
Ni 200 nm	Without	5	0	0	5
	873 K for 1 h	5	0	0	5
TiN 200 nm	Without	5	0	0	5
	873 K for 1 h	5	0	0	5

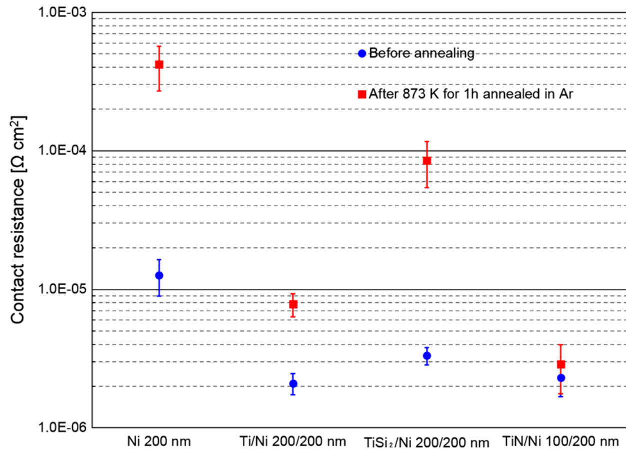

Fig. 5. Contact resistance before and after annealing of the samples at 873 K for 1 h in Ar.

Ti/Ni electrode, the contact resistance before annealing was low enough. Subsequently, the contact resistance increased after the sample had been annealed. Conversely, the contact resistance of the Ni and $TiSi_2$/Ni samples increased substantially. The wettability of InGa on the surface of the annealed Ti/Ni sample was not good and that on the annealed Ni and $TiSi_2$/Ni samples was poor. Mg apparently formed on the surface of Ni and was oxidized because no barrier existed on the Ni, Ti/Ni, or $TiSi_2$/Ni; the oxidized Mg then adversely affected the wetting properties of InGa. Therefore, we propose two explanations for the increase of the contact resistance of Ni and $TiSi_2$/Ni deposited on Mg_2Si:

1. an increase of the contact resistance between Ni and Mg_2Si, and $TiSi_2$ and Mg_2Si, and/or
2. an increase of the contact resistance between Ni and the RM-0.

We are currently uncertain which of these effects is the primary factor.

Mg never appeared on the electrode surface of the TiN film, as indicated by the measured low contact resistance after the sample was annealed. Our evaluation of the contact resistance indicates that the TiN barrier layer effectively prevents Mg diffusion.

CONCLUSION

Ti, $TiSi_2$, and TiN were selected as candidate materials for a barrier layer between Mg_2Si and Ni, and the barrier effect, adhesion, and contact resistance of each were evaluated. For TiN deposited on Mg_2Si, no Mg appeared on the TiN surface after annealing of the sample at 873 K for 1 h; in addition, the sample had a constant, low contact resistance. Weak long-term adhesion was observed for TiN on Mg_2Si. Here Ti is used as adhesion layer between the semiconductor substrate and TiN.[15] It is necessary to evaluate whether Ti can be used as an adhesion layer between TiN film and Mg_2Si. If the adhesion could be improved, TiN films would be a promising barrier layer.

ACKNOWLEDGEMENTS

The authors thank Yutaka Yabe, Shinichi Mizutani, Takefumi Yoshida, Naoki Sakaba (Showa Shinku Co., Ltd) for sample preparation, by use of sputtering equipment, and XPS analysis. This work was partly supported by the Future Pioneering Project “Research and Development of Thermal Management Materials and Technology” of the Japanese Ministry of Economy, Trade and Industry. The authors would like to thank Enago (www.enago.jp) for the English language review.

APPENDIX

Figure 6 shows the RM-0 device. The object being measured (e.g., a 2 × 2 × 2 mm^3 Mg_2Si TE chip) is placed between Au-plated Cu bars with contact via electrode surfaces formed on the object. The needle-type probe is located above the object. The Cu bars are connected to the AC current source of a Hioki BT3562. The cross-sectional area of the Cu bar is equal to that of the object, and the Cu bars and the object are electrically connected via liquid metal (In–Ga), to enable homogeneous flow of current through the object. The right Cu bar is also connected to the voltage-measurement terminal (+) of the BT3562, and this point of connection is

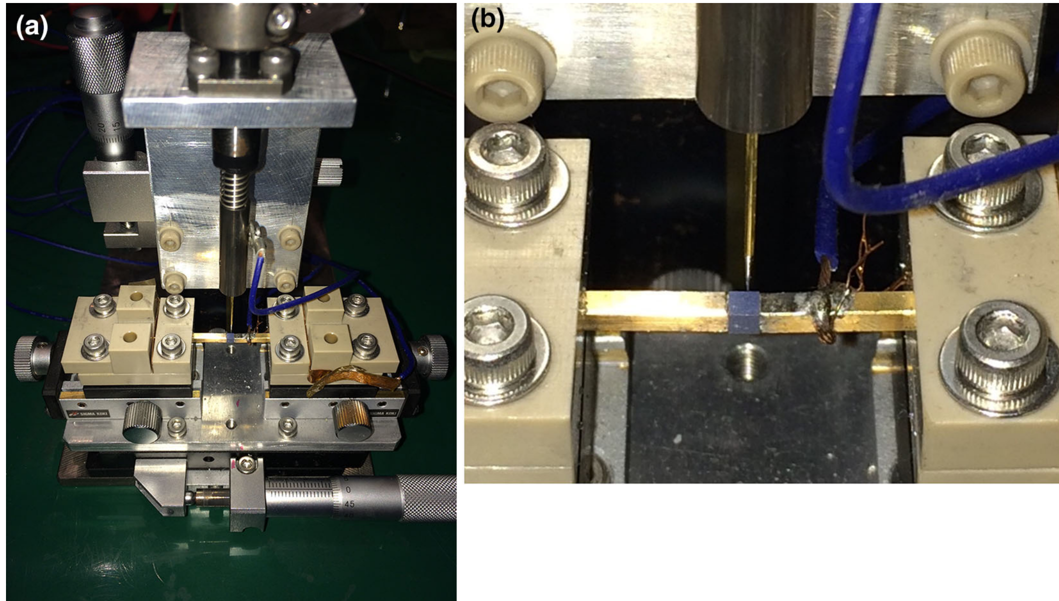

Fig. 6. Image of RM-0 device: (a) overview; (b) enlarged view.

determined as the origin of the resistance. The voltage-measurement terminal (−) is connected to the needle-type probe. This probe is able to move above the object and Cu blocks with 10-μm resolution. The position-dependent resistance increase is determined by intermittent needle scanning from right to left.

REFERENCES

1. http://romny-scientific.com/wp-content/uploads/2015/02/2014_Romny_IAV_Conference_condensed_color.pdf, p. 7. Accessed on April 2015.
2. J. de Boor, C. Gloanec, H. Kolb, R. Sottong, P. Ziolkowski, and E. Müller, *J. Alloys Compd.* 632, 348 (2015).
3. http://www.airia.or.jp/publish/statistics/ao1lkc00000000z4-att/03_32.pdf. Accessed on May 2015.
4. T. Sakamoto, T. Iida, Y. Honda, M. Tada, T. Sekiguchi, K. Nishio, Y. Kogo, and Y. Takanashi, *J. Electron. Mater.* 41, 1805 (2012).
5. B.L. Sharma, *Diffusion in Semiconductors* (Trans. Tech. Pub. Germany, 1970), p. 87.
6. S. Hocine and D. Mathiot, *Appl. Phys. Lett.* 53, 1269 (1988).
7. http://www.crct.polymtl.ca/fact/phase_diagram.php?file=Mg-Ti.jpg&dir=FTlite. Accessed on May 2015.
8. Y. Nakamura, H. Nakajima, S. Ishioka, and M. Koiwa, *Acta Metall.* 36, 2787 (1988).
9. M. Bhaskaran, S. Sriram, D.R.G. Mitchell, and A.S. Holland, *Semicond. Sci. Technol.* 23, 035021 (2008).
10. S. Zhang and M. Östling, *Crit. Rev. Solid State Mater. Sci.* 28, 1 (2003).
11. http://www.globalsino.com/EM/page150.html. Accessed on May 2015.
12. Y. Nishi and R. Doering, eds., *Handbook of Semiconductor Manufacturing Technology (in Section 10)*, 2nd ed. (Boca Raton: CRC Press, 2007), pp. 18–21.
13. C.Y. Ting and M. Wittmer, *Thin Solid Films* 96, 327 (1982).
14. K.G. Grigorov, G.I. Grigorov, M. Stoyanova, J.-L. Vignes, J.-P. Langeron, P. Denjean, and J. Perriere, *Appl. Phys. A* 55, 502 (1992).
15. S. Sugimoto, T. Kamigaki, and H. Kamijo, *Toshiba Rev.* 59, 7 (2004).
16. M.Y. Kwak, D.H. Shin, T.W. Kang, and K.N. Kim, *Thin Solid Films* 339, 290 (1999).
17. T. Sakamoto, T. Iida, Y. Ohno, M. Ishikawa, Y. Kogo, N. Hirayama, K. Arai, T. Nakamura, Y. Nishio, and Y. Takanashi, *J. Electron. Mater.* 43, 1620 (2014).
18. S. Ohara, *Kinzoku zairyou gairon (Summary of Metal Materials)* (Tokyo: Asakura Publishing, 1991), pp. 280–281.
19. L. Szparaga, J. Ratajski, and A. Zarychta, *Arch. Mater. Sci. Eng.* 48, 35 (2011).